# Wavelet-based fractal signature analysis for automatic target recognition

**Fausto Espinal**
**Terrance Huntsberger,** MEMBER SPIE
University of South Carolina
Department of Computer Science
Intelligent Systems Laboratory
Columbia, South Carolina 29208
E-mail: espinal@cs.sc.edu

**Björn D. Jawerth**
University of South Carolina
Industrial Mathematics Initiative
Department of Mathematics
Columbia, South Carolina 29208

**Toshiro Kubota**
University of South Carolina
Department of Computer Science
Intelligent Systems Laboratory
Columbia, South Carolina 29208

**Abstract.** Texture measures offer a means of detecting targets in background clutter that has similar spectral characteristics. Our previous studies demonstrated that the ''fractal signature'' (a feature set based on the fractal surface area function) is very accurate and robust for gray-scale texture classification. This paper introduces a new multichannel texture model that characterizes patterns as 2-D functions in a Besov space. The wavelet-based fractal signature generates an $n$-dimensional surface, which is used for classification. Results of some experimental studies are presented demonstrating the usefulness of this texture measure. 
[S0091-3286(98)01001-0]

Subject terms: recognition techniques; wavelets; fractal dimension; texture analysis; segmentation; targeting.

Paper ART-123 received June 2, 1997; revised manuscript received Aug. 19, 1997; accepted for publication Aug. 21, 1997.

## 1 Introduction

The accurate detection and discrimination of texture remains one of the most fundamental problems in computer vision. Regardless of whether the application is target detection, object recognition, texture segmentation, or edge detection, we must be able to recognize and label homogeneous texture regions within an image and differentiate between distinct regions. We can safely state that scene segmentation is one of the most important and fundamental tasks of early vision. Moreover, the solution to many vision-related problems depend on an efficient image segmentation to arrive at correct solutions. Thus the development of accurate texture description models is crucial for the solution of these problems. The texture measure presented in this paper, which we call the wavelet-based fractal dimension, is a promising alternative to current texture measures and overcomes some of their limitations.

## 2 Background

The computational processing of textures can be divided into two main problem areas, segmentation and classification. Texture classification consists of taking whole images and grouping them into texture classes or categories, so as to be able to rapidly detect whether two texture samples are alike or dissimilar. Texture segmentation is, on the other hand, the process by which an image is partitioned into regions of homogeneous texture patterns. Segmentation is a more complex problem than classification since it involves discriminating textures and being able to tell them apart. But it also involves the optimal detection of boundaries between nonhomogeneous texture regions.

### 2.1 *Texture Metrics*

Two questions that arise from the previous definitions are what is meant by homogeneous or dissimilar texture regions and how this can be expressed quantitatively. The answer to the first question is obvious due to the fact that for humans it is natural and easy to classify textures or to segment textured images into homogeneous regions. Therefore this should be the standard that determines the homogeneity of two textures. The second question, on the other hand, does not have a straightforward answer. Computer vision researchers have for many years attempted to model the basic components of the human visual system to capture our visual abilities. As a result of these efforts, several models have risen to try and measure quantitatively the intrinsic and unique properties of texture patterns. Most of these models consist of mapping texture patterns to an $n$-dimensional feature space from which some labeling technique can be applied to determine which texture patterns can be categorized as similar or not similar.

Statistical modeling approaches for textures are quite popular. Stationary statistical models are used to calculate parameters that are unique to each texture's pixel value distribution. Typical models used are nonlinear Markov random fields[1] (MRFs) and Gauss MRFs.

Probably the most popular approach to quantizing texture properties is currently the usage of Gabor filters to perform feature extraction. Gabor filters are modulated sinusoids of the form

$$G(x,\sigma,A)=\frac{1}{(2\pi\sigma)^{1/2}}\exp(-x^2/2\sigma)e^{iAx}, \tag{1}$$

where $A$ is the frequency of the sinusoid and $\sigma$ determines the width of the Gaussian envelope. These filters are known to have good discrimination capabilities for many types of textures. References 2 to 9 use Gabor filtering as their tex-

ture metric of choice. The elements of the feature vectors created represent the energy of the texture at a particular frequency and orientation.

Wavelets are very much related to Gabor filters in that they provide localized space-frequency information for a signal. In particular, 2-D wavelet transforms provide frequency and orientation content information for 2-D signals. Wavelets have to the advantage that they partition the frequency plane precisely, unlike Gabor filters. But, Gabor filters provide complete control over orientation unlike the more limited control offered by 2-D separable wavelet transforms. Wavelet-based methods for texture modeling and feature extraction have generally focused on the utilization of the packets or frames of the Wavelet transform and using these to obtain features with which to classify or segment a textured image. References 10 and 11 are good examples of these methods.

This paper introduces a novel texture metric that can be used for classification, segmentation, or target recognition based on the fractal dimension and the 2-D wavelet transform. The wavelet-based fractal dimension provides a fast feature extraction method that results in very good texture discrimination capabilities.

## 3 Wavelet-Based Fractal Dimension

### 3.1 *Fractal Signature*

Texture measures offer a means of detecting objects in background clutter that has similar spectral characteristics. The ''fractal signature'' (a feature set based on the fractal surface area function) was shown to be very accurate and robust in gray-scale texture classification.[12–14] The strength of applying fractal theory to texture analysis lies in the multiresolution nature of texture, which is the basis of fractals.

Peleg et al.[14] introduced a texture analysis method that measures the area of the gray-level surface at varying resolutions. For a pure fractal gray-level image, this is given by

$$A(\epsilon)=F\epsilon^{(2-D)}, \tag{2}$$

where $\epsilon$ is the resolution of the gray levels in the image, $D$ is a fractal dimension,[15] and $F$ is a constant. The change in measured area with the changing scale is used as the fractal signature of the texture. The gray-level surface area is measured by covering the surface in 3-D space with a blanket of thickness $2\epsilon$, whose upper surface and lower surface are derived using local max and min functions applied to the image. The surface area can be computed from the volume occupied by the blanket. This will give a measure of the oscillations of the underlying surface for each value of $\epsilon$, which is used to generate the fractal signature.

Argoul et al.[16] were the first to propose the use of the wavelet transform for fractal image description. They used the transform as a microscope to capture the scaling properties of fractals. Mallat has shown that texture analysis can be done with the wavelet representation using a fractal dimension derived from the power function spectra.[17] This type of analysis can be merged with the fractal signature approach.[12,13] Although the fractal signature can be computed in parallel, there is a large computational overhead in the max and min functions that are the basis for the convex hull support of the image surface. An alternative and much more efficient approach lies in the computation of a fractal dimension within the $\gamma$ wavelet coefficient spaces where a measure of texture directionality is also obtained. In addition, multichannel texture models can be built using the method found in Ref. 13.

### 3.2 *Definition of the Wavelet-Based Fractal Dimension*

The fractal dimension of a compact set $E$ is given by

$$\dim(E)=\lim_{\epsilon\to\infty}\frac{\log \mathcal{N}(\epsilon,\mathcal{E})}{\log(1/\epsilon)}, \tag{3}$$

where $\mathcal{N}(\epsilon,E)$ is the number of balls of radius $\epsilon$ that cover the set $E$. This measure gives a rudimentary geometric description of a set and how complicated it looks. Thus it intuitively lends itself to consideration as an accurate texture metric. See Refs. 18 and 19 for more details on the mathematical properties of the fractal dimension.

Humans cue to many features when segmenting a scene. One such feature is the degree of smoothness that a pattern demonstrates. Thus we can use this feature to try and measure a texture quantitatively. From the field of functional analysis it is known that functions can be categorized by their degrees of smoothness. Functions can be categorized into functional spaces according to their degrees of smoothness. Besov spaces offer one such way to classify functions by their mathematical smoothness, which is very close to our notion of visual smoothness.

Define $\varphi$ to be the space of functions belonging to $C^{\infty}$ that decay rapidly at $\infty$. A Besov space $B_p^{\alpha,q}(R)$ is the collection of all functions $f\in\varphi$ such that

$$\|f\|_{B_p^{\alpha,q}(R)}=\|\Phi*f\|_{L^p}+\left[\sum_{\nu=1}^{\infty}(2^{\nu\alpha}\|\psi_\nu*f\|_{L^p})^q\right]^{1/q}<\infty, \tag{4}$$

where $\alpha\in\Re$, $1\leqslant p\leqslant\infty$ and $1\leqslant q\leqslant\infty$. Here $\psi_\nu=2^\nu\psi(2^\nu x)$ is a wavelet-like function that decays at infinity formed by dilations of the basic function $\psi$, and $\Phi\in\varphi$ is a smooth scaling function. The Besov space norm measures how smooth a function is. If the norm of $f$ is high, it indicates the presence of many high-frequency components in $f$ and thus a non-smooth function. See Refs. 18 and 19 for more details on the mathematical properties of Besov spaces.

The results in Ref. 18 show that a fractal dimension of the graph of $f\in B_p^{\alpha,q}(R)$ can be expressed using its wavelet coefficients. In other words, the smoothness of a function is intrinsically connected to the geometric characteristic of the graph of that function and hence to its fractal dimension.

The dyadic wavelet transform of a function $f\in L^2(\Re)$ is given by*

*See Ref. 20 for more a more complete introduction to the wavelets and multiresolution analysis.

$$(\mathscr{W}_{\nu} f)(b,\nu) := \frac{1}{\sqrt{2^{\nu}}} \int_{-\infty}^{\infty} f(x)\psi\left(\frac{x-b}{2^{\nu}}\right) dx, \tag{5}$$

where $\psi(x)$ is typically referred to in the literature as the mother wavelet and is a compactly supported function that decays rapidly to zero at infinity. This transform is useful in providing localized space-frequency information within certain frequency scales of a function and can also be interpreted as providing smoothness information:

$$\dim[\text{graph}(f)] = \lim_{\nu\to\infty} \frac{\log^{+} \Sigma_{|I|=2^{-\nu}} |I|^{-1/2} |[\mathscr{W}_{\nu}(f)]_I|}{\log^{+} 2^{\nu}} + 1, \tag{6}$$

where $[\mathscr{W}_{\nu}(f)]_I$ are the wavelet coefficients of the function $f$ in the dyadic interval $I$, where $|I| = 2^{-\nu}$. For a 2-D function $f:[0,1]^2 \to \Re$, we must use the 2-D separable wavelet transform given by

$$(\mathscr{W}_{\nu,\theta} f)(a,b): = \frac{1}{\sqrt{2^{\nu}}} \int_{-\infty}^{\infty}\int_{-\infty}^{\infty} f(x,y)\psi_{\theta}\left(\frac{x-a}{2^{\nu}}, \frac{y-b}{2^{\nu}}\right) dx\, dy. \tag{7}$$

The wavelet $\psi_{\theta}$ is one of the three possible mother wavelets that extract horizontal, diagonal,or vertical orientation information from the function $f(x,y)$. Using this definition, we can extend the fractal dimension equation to 2-D functions $f(x,y)$:

$$\dim[\text{graph}(f)] = \lim_{\nu\to\infty} \frac{\log^{+} \Sigma_{|A|=2^{-2\nu}} |A|^{-1/2} |[\mathscr{W}_{\nu,\theta}(f)(a,b)]|}{\log^{+} 2^{\nu}} + 1, \tag{8}$$

where $\theta$ denotes which of the horizontal, vertical, or diagonal channels of the 2-D wavelet transform the coefficients belong to, and $A$ is analogous to $I$ except that it is a 2-D patch of area $|A| = 2^{-2\nu}$. Thus we can think of the 2-D wavelet-based fractal dimension for a function $f:[0,1]^2 \to \Re$ as a vector belonging to $\Re^3$ corresponding to the three different orientations of the wavelet transform.

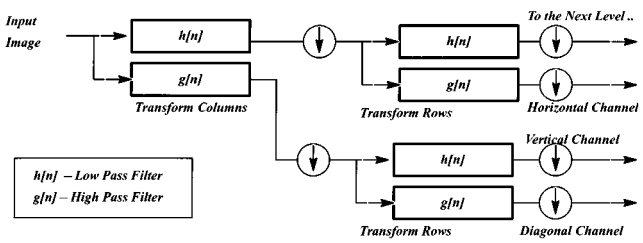


**Fig. 1** Computational structure of a discrete wavelet transform; $h[n]$ and $g[n]$ are low-pass and high-pass filters, respectively. Three orientation channels are the output of each level of decomposition.

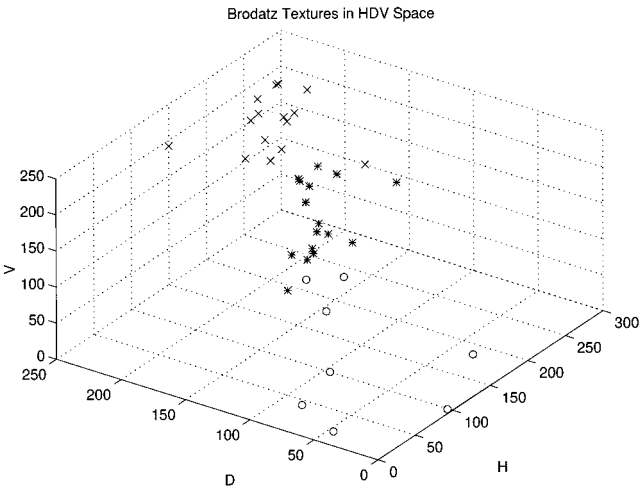


**Fig. 2** Sample of 40 Brodatz-like textures in HDV space.

## 4 Implementation of the Wavelet-Based Fractal Dimension

To use the fractal dimension as a feature metric, we must compute it for signals of finite length, i.e., digitized images. The fact that we are dealing with discrete signals means that we do not have infinite levels of resolution. This means we only have a finite number of values $\nu$ with which to try and approximate this limit. Thus we will use the sequence of values given by different values of $\nu$ and the different orientations as a feature vector for the image subregion for which we are trying to compute a fractal dimension.

We evaluate and compute for each image pixel the following formula:

$$D_{\theta,\nu}(p) = \frac{\log^{+}\{\Sigma_{u\in\mathscr{W}_{\theta,\nu}[\mathscr{N}(p)]} |u| \sqrt{2^{-\nu}}\}}{\log^{+}(2^{\nu})}, \tag{9}$$

where $\mathscr{N}(p) \in \Re^{m\times m}$ is the image subwindow surrounding pixel $p$ representing the function for which we are computing a fractal dimension, and $\nu \in \{0,...,\log_2 m\}$ are the levels of resolution of the discrete wavelet transform of the subimage. Figure 1 shows the basic steps of iterative filtering and downsampling involved in computing the discrete wavelet transform of a 2-D signal.

To visualize the discrimination properties of our proposed metric, we computed the wavelet-based fractal dimension for 40 patches of Brodatz-like texture samples and averaged them for each orientation channel. Figure 2 shows the results of the plot in HDV space† for the 40 Brodatz-like textures in Fig. 3.

## 5 Experimental Results

We performed two basic types of experiments to test the applicability of our texture metric. We first used it to do simple image segmentation and compare our image results to the commonly used Gabor filter metrics. Then we proceeded to use them in targeting experiments from which we also show the resulting images.

†Horizontal, diagonal, and vertical channels of the 2-D wavelet transform.

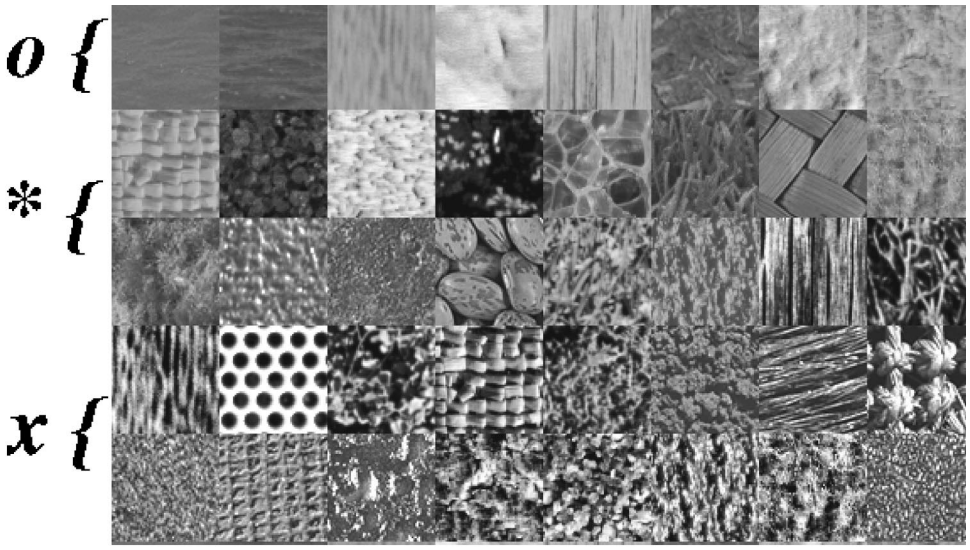

**Fig. 3** Collage of 40 Brodatz-like textures.

### 5.1 *Application to Segmentation*

To test the discrimination ability of the wavelet-based fractal dimension, we decided to compare its feature extraction abilities to Gabor filters. For our experiments we used a test set of $256\times256$ 8-bit images composed of different texture patches taken from the work done in Refs. 3 and 4. For each image, we computed the wavelet-based fractal dimension feature vectors using either a $16\times16$ or a $32\times32$ window size and using the coefficients of up to the first three levels of the discrete wavelet transform decomposition. The number of levels of the wavelet transform used in the feature extraction depended on the window size used; that is, for smaller window sizes, a smaller number of levels of the transform were utilized due to the more limited resolution. It is important to note that these window sizes depend on the size of the textures being analyzed and they were determined manually. For all of our experiments we used the five-tap biorthogonal wavelet shown[21] in Table 1. We also extracted features using Gabor filters for four different orientations and three different center frequencies followed by a pixelwise nonlinear transform and the local absolute averaging described in Ref. 22. We proceeded to segment both feature sets using the simple and well-known *k*-means clustering technique,[23] using the feature vectors only and no spatial coordinate information. We observed in general that our feature metric differentiated better between visually close textures than the Gabor filters. This result is even more interesting when we take into account the fact that the dimensionality of our feature space was at most 9 while the Gabor metric was 12. So while the running times of the feature extraction procedures are about the same, the clustering algorithm module will undoubtedly take longer for a feature space of higher dimensionality.

**Table 1** Coefficients for the low-pass and high-pass filters of the biorthogonal wavelet used in the experiments.

| | |
|---|---|
| Low-pass filter | 0.353553, 0.707107, 0.353553 |
| High-pass filter | −0.176777, 0.353553, 1.06066, 0.353553, −0.176777 |

Figure 4 demonstrates that the fractal-signature-based method is able to differentiate better between the woolen cloth (center) and the water (far right). It is interesting to observe that the border between these two textures is not very clear and the fractal-based features are able to detect it. The Gabor filters also were too sensitive to the wood texture at the bottom and thus over segmented it. Figure 5 shows that our metric is better at distinguishing between the water and the pigskin texture. The borders of the perforated metal (center) are also much better localized. The speckles in our segmentation results show that our metric is quite sensitive to noise. But these limitations can be overcome through the use of more sophisticated clustering approaches like the ones in Refs. 1, 3, and 4.

The results in Fig. 6 show again that Gabor filters could not differentiate between two similar textures, the water in the center and the particle board at the bottom. It can be observed in this image that the border between these two textures is not readily discernible and our metric is also affected. The metal texture at the top is oversegmented by the Gabor filters, probably due to the overall change in brightness across the texture. Figure 7 shows some more speckle noise in the segmentation image of the wavelet-based fractal signature. But the Gabor filter output creates large spots in several of the textures due to brightness changes in the textures.

The segmentation results in Fig. 8 shows almost identical output from both our metric and Gabor filters. The most obvious differences are the better circle edge localization and more speckle noise in our metric segmentation. Figure 9 shows a more clean segmentation using Gabor filters than our metric. The poor boundary detection between the woolen cloth (left) and the coarse sand (bottom) is most probably due to their very close proximity in HDV space (see Fig. 3).

Figure 10 shows the percentage of mislabeled pixels for each of the wavelet-based fractal dimension segmentations. Note again that we are not utilizing a sophisticated cluster-

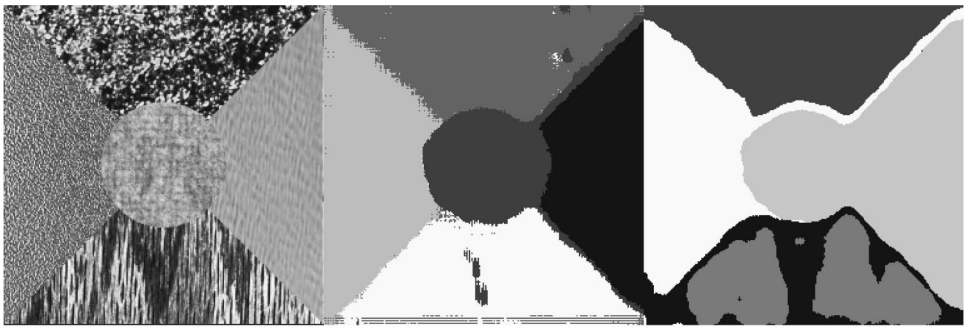

(a) (b) (c)

**Fig. 4** (a) Test image 1, (b) segmentation result using wavelet-based fractal dimension features (using window size of 16×16 and first two levels of wavelet transform decomposition), and (c) segmentation result using Gabor filter features with four orientations and three center frequencies.

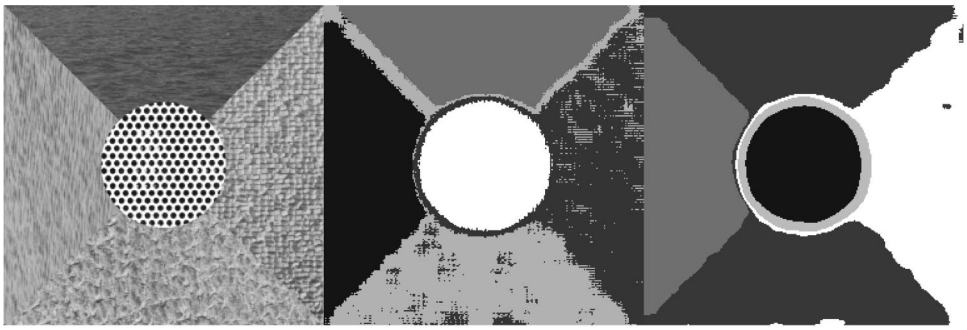

(a) (b) (c)

**Fig. 5** (a) Test image 2, (b) segmentation result using wavelet-based fractal dimension features (using window size of 16×16 and first two levels of wavelet transform decomposition), and (c) segmentation result using Gabor filter features with four orientations and three center frequencies.

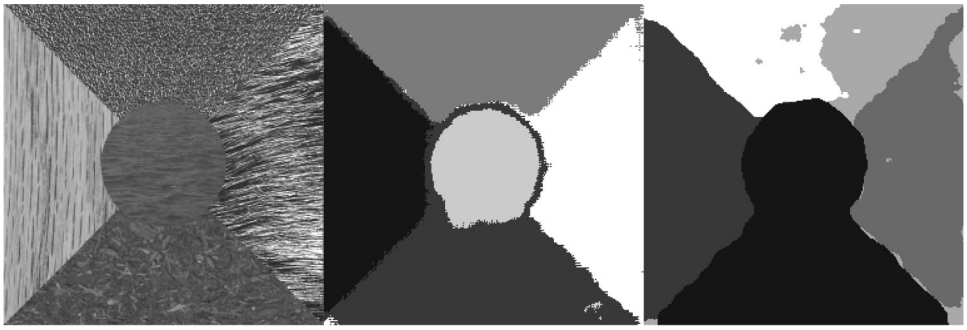

(a) (b) (c)

**Fig. 6** (a) Test image 3, (b) segmentation result using wavelet-based fractal dimension features (using window size of 16×16 and first two levels of wavelet transform decomposition), and (c) segmentation result using Gabor filter features with four orientations and three center frequencies.

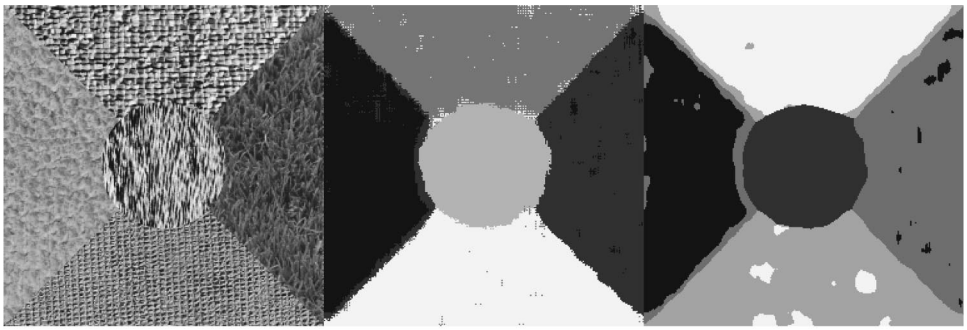

(a) (b) (c)

**Fig. 7** (a) Test image 4, (b) segmentation result using wavelet-based fractal dimension features (using window size of 16×16 and first two levels of wavelet transform decomposition), and (c) segmentation result using Gabor filter features with four orientations and three center frequencies.

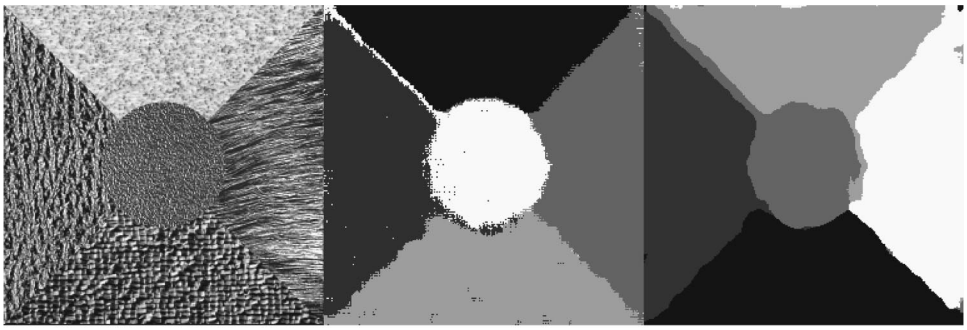

(a) (b) (c)

**Fig. 8** (a) Test image 5, (b) segmentation result using wavelet-based fractal dimension features (using window size of 16×16 and first two levels of wavelet transform decomposition), (c) segmentation result using Gabor filter features with four orientations and three center frequencies.

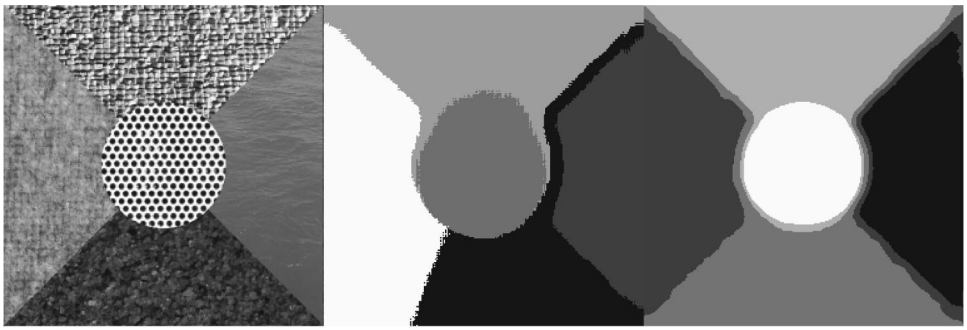

(a) (b) (c)

**Fig. 9** (a) Test image 6, (b) segmentation result using wavelet-based fractal dimension features (using window size of 32×32 and first two levels of wavelet transform decomposition), and (c) segmentation result using Gabor filter features with four orientations and three center frequencies.

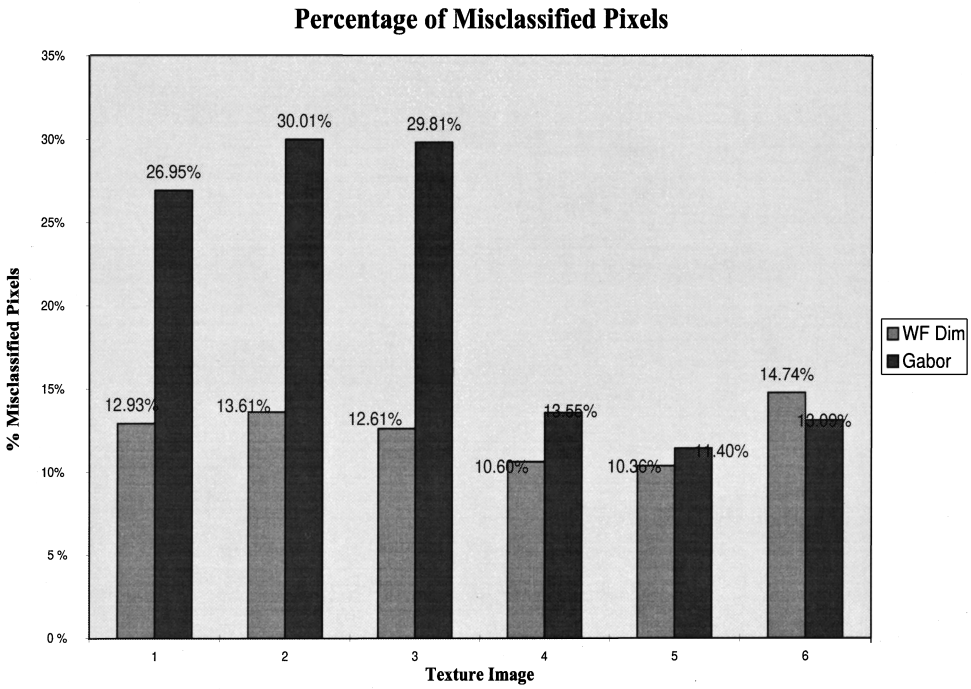


**Fig. 10** Pixel error percentage results for the six segmentation examples.

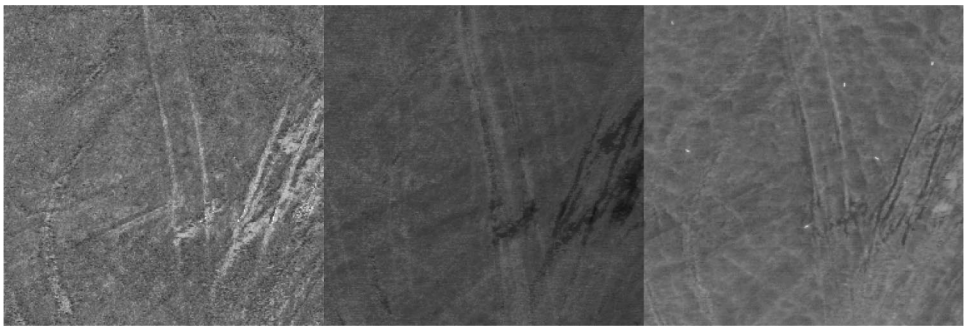

**Fig. 11** Polarization, reflectance, and thermal IR band image.

ing technique. Better results can be obtained by incorporating spatial constraints into the clustering technique by discouraging small blocks of homogeneous pixels. Energy minimization techniques like simulated annealing can accomplish this but are very computationally intensive. The authors of Refs. 3 and 4 have overcome some shortcomings of this energy minimization method.

### 5.2 *Automatic Target Detection*

Our studies with the texture mosaics revealed the link between the wavelet-based fractal signature and the smoothness of a texture. Man-made objects such as targets tend to be characterized by linear/angular features that show up well in the wavelet detail channels, thus leading to relatively high values for the signature at every scale. The fractal signature of the target will be mixed with that of the background clutter, but to the first order this will be a additive mixing of signatures.[24]

All images had a spatial resolution of $512\times512$ pixels and 8 bits of gray scale. Although targets are made up of a number of different textures, their combination should give a unique signature. Rather than deriving a signature for each pixel, as was done in the mosaic study, we derived signatures for larger windows that encompass the target.

In the first study, we used a series of registered images that were taken in the polarization, reflectance and thermal IR bands shown in Fig. 11. The targets are small cylindrical objects that are partially embedded in the ground.

The total area of the targets with respect to the field of view (FOV) was 0.05%. In addition, their spectral signatures were extremely close to that of the vehicular tracks that were also present. An approach based on thresholding yielded a probability of false alarm $P_{\mathrm{FA}}$ of 34% without further processing. Analysis of the thermal band using the fractal signature derived from the $\gamma$ channels of the biorthogonal closed set wavelet transform with an image decomposition of 64 subimages gave a probability of detection $P_D$ of 83% for a $P_{\mathrm{FA}}$ of 0%, and a $P_D$ of 100% with a $P_{\mathrm{FA}}$ of 10%. Classification accuracy of the algorithm is slightly increased if the polarization and thermal images are fused using a possibilistic OR operation in the $\gamma$ channels before texture analysis. This method produced a $P_D$ of 100% with a $P_{\mathrm{FA}}$ of 7% and compares favorably with a previously reported neural-network-based technique.[25]

In the second study, we used a series of images from the China Lake thermal IR database. These include both land and nautical examples. The target signatures are known within bandpass limits in the three detail channels. A fixed size window of size $4\times4$ is used to scan the input image in the lowest level of the wavelet coefficient space using the texture measure previously defined in this paper. This is followed by a simple region-growing process, which gives rise to the bounding rectangle around the target.

The first series had land targets hidden in vegetation and a target without any cover. These are shown in Fig. 12,

**Fig. 12** Land target examples.

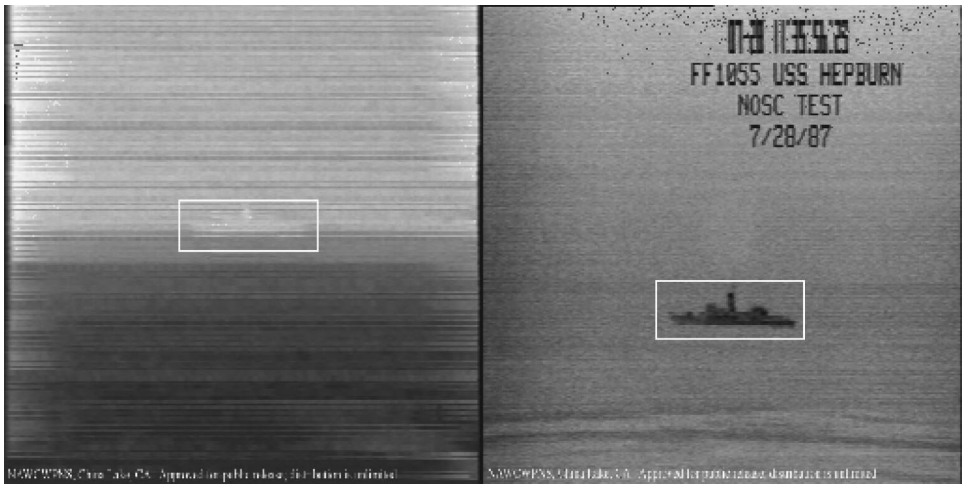


**Fig. 13** Sea target examples: (a) hot horizon target and (b) target without any cover.

where we have boxed the detected targets in each scene. Despite the high amount of clutter in each scene, the targets were successfully detected. The second series had a nautical target hidden in the ''hot'' horizon and a target without any cover. These are shown in Fig. 13, where we have boxed the detected targets in each scene. The target in the left image was detected despite extremely low contrast between itself and the sky return.

## 6 Conclusions and Future Work

Clearly the wavelet-based fractal dimension offers a new and promising way to measure texture features. Its ability to distinguish boundaries between textures that even for humans are not clear indicates that it is able to cue into properties of textures that are hard for us to detect.

In all of our experiments, we empirically set the number of levels of the wavelet decomposition to use and the respective window sizes. This, of course, is not the most efficient approach. For most images a window size of 16 $\times$16 and information from the first two levels of the wavelet decomposition were used for feature extraction. But for larger sized textures, such as beans or woven thatch, a larger window size proved more effective. Thus an adaptive approach that determines the optimal value for these two parameters would be desirable.

### *Acknowledgments*

Fausto Espinal's research is supported under Army Research Office (ARO) Contract no. DAAH04-96-10326. Terry Huntsberger was supported under ARO Contract no. DAAH04-96-10326 and Office of Naval Research (ONR) Contracts nos. N00014-94-1-1163 and DAAH04-95-C-003. Björn Jawerth was supported under ARO Contract no. DAAH04-96-10326, ONR Contracts nos. N00014-94-1-1163, DAAH04-95-C-003, and ARPA\DEPSCOR 36197RTDPS. Toshiro Kubota was supported under ARO Contract no. DAAH04-96-10326 and ONR Contract no. N00014-94-1-1163. The authors wish to thank all of these agencies for their continued support.

### *References*

1. C. Kervrann and F. Heitz, ''A Markov Random Field model-based approach to unsupervised texture segmentation using local and global spatial statistics,'' *IEEE Trans. Image Process.* **4**(6), 856–862 (1995).
2. T. S. Lee, ''A Bayesian framework for understanding texture segmentation in the primary visual cortex,'' *Vis. Res.* **35**(18), 2643–2657 (1995).
3. T. Hofmann, J. Puzicha, and J. M. Buhmann, ''Unsupervised segmentation of textured images by pairwise data clustering,'' in *Proc. IEEE Int. Conf. on Image Processing*, Vol. 3, pp. 137–140, Laussanne (1996).
4. T. Hofmann, J. Puzicha, and J. M. Buhmann, ''Deterministic annealing for unsupervised texture segmentation,'' in *Lecture Notes in Computer Science: Proc. Int. Workshop on Energy Minimization Methods in Computer Vision and Pattern Recognition*, pp. 213–228, Venice, Springer-Verlag, Berlin (1997).
5. R. Azencott, J. Ping, and L. Younes, ''Texture classification using windowed Fourier filters,'' *IEEE Trans. Pattern Anal. Mach. Intell.* **19**(2), 148–153 (1997).
6. A. Teuner, O. Pichler, and B. J. Hosticka, ''Unsupervised texture segmentation of images using tuned matched Gabor filters,'' *IEEE Trans. Image Process.* **4**(6), 863–870 (1995).
7. A. C. Bovic, M. Clark, and W. S. Geisler, ''Multichannel texture analysis using localized spatial filters,'' *IEEE Trans. Pattern Anal. Mach. Intell.* **12**(1), 55–73 (1990).
8. D. Dunn, W. Higgins, and J. Wakeley, ''2-D analysis of Gabor-filter output signatures for texture segmentation,'' in *Proc. IEEE Int. Conf. Acoust. Speech Sig. Proc. 92*, Vol. 3, pp. 65–68 (1992).
9. O. Pichler, A. Teuner, and B. J. Hosticka, ''A comparison of texture feature extraction using adaptive Gabor filtering, pyramidal and tree structured wavelet transforms,'' *Pattern Recog.* **29**(5), 733–742 (1996).
10. A. Laine and J. Fan, ''Texture classification by wavelet packet signatures,'' *IEEE Trans. Pattern Anal. Mach. Intell.* **15**(11), 1186–1191 (1993).
11. A. Laine and J. Fan, ''An adaptive approach for texture segmentation by multi-channel wavelet frames,'' Technical Report TR-93-025, Center for Computer Vision and Visualization, Univ. of Florida, Gainesville, FL (Aug. 1993).
12. B. A. Huntsberger, S. N. Jayaramamurthy, and T. L. Huntsberger, ''Morphological classification of color textures,'' in *Proc. IEEE 30th Midwest Symp. on Circuits and Systems*, pp. 363–366, Syracuse, NY (1987).
13. B. A. Huntsberger and T. L. Huntsberger, ''Hypercube algorithms for multi-spectral texture analysis,'' in *Proc. 4th Conf. on Hypercube Concurrent Computers and Applications (HCCA4)*, pp. 1009–1012, Golden Gate Enterprises, Los Altos, CA (1989).
14. S. Peleg, J. Naor, R. Hartley, and D. Avnir, ''Multiple resolution texture analysis and classification,'' *IEEE Trans. Pattern Anal. Mach. Intell.* **6**, 518–523 (1984).
15. B. B. Mandelbrot, *The Fractal Geometry of Nature*, W. H. Freeman, San Francisco (1982).
16. F. Argoul, A. Arneodo, J. Elezgaray, and G. Grasseau, ''Wavelet transform of fractal aggregates,'' *Phys. Lett. A* **135**(6,7), 327–335 (1989).
17. S. Mallat, ''A theory for multiresolution signal decomposition: the wavelet representation,'' *IEEE Trans. Pattern Anal. Mach. Intell.* **11**, 674–693 (1989).
18. A. Deliu and B. Jawerth, ''Geometrical dimension versus smoothness,'' *Construct. Approx.* **8**, 211–222 (1992).
19. P. Brenner, V. Thomee, and L. B. Wahlbin, *Besov Spaces and Appli-*

*cations to Difference Methods for Initial Value Problems*, Lecture Notes in Mathematics, Number 434, Springer-Verlag, Berlin.
20. C. K. Chui, *An Introduction to Wavelets*, Academic Press, New York (1992).
21. J. D. Villasenor, B. Belzer, and J. Liao, ''Wavelet filter evaluation for image compression,'' *IEEE Trans. Image Process.* **4**(8), 1053–1060 (1995).
22. A. K. Jain and F. Farrokhia, ''Unsupervised texture segmentation using Gabor filters,'' in *Proc. IEEE Int. Conf. on Systems, Man and Cybernetics*, pp. 14–19 (1990).
23. J. T. Tou and R. C. Gonzalez, *Pattern Recognition Principles*, Addison-Wesley, Reading, MA (1974).
24. J. Hu, S. N. Jayaramamurthy, and T. L. Huntsberger, ''Fractal signature analysis of mixtures of textures,'' in *Proc. IEEE S.E. Symp. Systems Theory*, pp. 32–35, Clemson, SC (1987).
25. T. L. Huntsberger, ''Biologically motivated cross-modality sensory fusion system for automatic target recognition,'' *Neural Net.* **8**(7/8) 1215–1226 (1995).

**Fausto Espinal** received his BS in systems engineering and computation from the Pontificia Universidad Catolica Madre y Maestra, Dominican Republic, in 1992. He is currently a research assistant and PhD candidate in the Department of Computer Science at the University of South Carolina. His research interests include computer vision, computer graphics, image processing, and wavelet applications to these fields.

**Terrance Huntsberger:** Biography and photograph appear with the paper ''Wavelet-based system for recognition and labeling of polyhedral junctions'' in this issue.

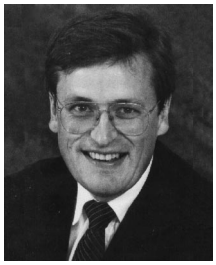

**Björn D. Jawerth** received an MSc in mathematics and statistics, an MSc in physics, and a PhD in mathematics in 1977, all from the Lund Institute of Technology, Sweden. He is the David M. Robinson Professor of Mathematics at the University of South Carolina, where he directs the Industrial Mathematics Initiative. Dr. Jawerth is also CEO of Summus Ltd., a company specializing in image and video compression and related wavelet technologies. His research interests include harmonic analysis and partial differential equations with computational applications.

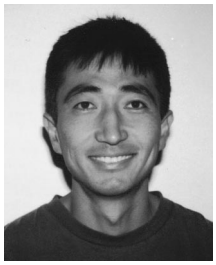

**Toshiro Kubota** received his BS degree in instrumentation engineering from Keio University in 1988 and MSEE and PhD degrees in electrical and computer engineering from Georgia Institute of Technology in 1989 and 1995, respectively, where from 1989 to 1995, he was a research assistant in the Computer Engineering Research Laboratory. In 1996, he became a lecturer and research associate in the Department of Computer Science, University of South Carolina. His current research interests include computer vision, biological vision, neural networks, parallel processing, and visualization.